Rapid Communications

Comparing all-optical switching in synthetic-ferrimagnetic multilayers and alloys

M. Beens [1,*] M. L. M. Lalieu [1] A. J. M. Deenen [1] R. A. Duine [1,2] and B. Koopmans [1]

[1]*Department of Applied Physics, Eindhoven University of Technology, P.O. Box 513, 5600 MB Eindhoven, The Netherlands*

[2]*Institute for Theoretical Physics, Utrecht University, Leuvenlaan 4, 3584 CE Utrecht, The Netherlands*

(Received 31 July 2019; revised manuscript received 16 October 2019; published 26 December 2019)

We present an experimental and theoretical investigation of all-optical switching by single femtosecond laser pulses. Our experimental results demonstrate that, unlike rare-earth transition-metal ferrimagnetic alloys, Pt/Co/$[Ni/Co]_N$/Gd can be switched in the absence of a magnetization compensation temperature, indicative for strikingly different switching conditions. In order to understand the underlying mechanism, we model the laser-induced magnetization dynamics in Co/Gd bilayers and GdCo alloys on an equal footing, using an extension of the microscopic three-temperature model to multiple magnetic sublattices and including exchange scattering. In agreement with our experimental observations, the model shows that Co/Gd bilayers can be switched for a thickness of the Co layer far away from compensating the total Co and Gd magnetic moment. We identify the switching mechanism in Co/Gd bilayers as a front of reversed Co magnetization that nucleates near the Co/Gd interface and propagates through the Co layer driven by exchange scattering.

DOI: 10.1103/PhysRevB.100.220409

Femtosecond laser pulses provide a unique tool to manipulate magnetic order on ultrashort timescales. A prime example of this is all-optical switching (AOS) of magnetization by a single pulse, as first observed in ferrimagnetic GdFeCo alloys using circularly polarized laser pulses [1]. Later, AOS was demonstrated in the same material by using a single linearly polarized laser pulse [2,3], which indicated that GdFeCo can be switched with ultrafast heating as the only stimulus.

Deterministic AOS has a potential to be used in future magnetic memory devices, offering an ultrafast and energy-efficient way to write data. Helicity-dependent AOS by circularly polarized pulses has been demonstrated in a wide variety of materials [4–6]. However, in those cases the switch follows from a multiple-pulse mechanism. Purely thermal single-pulse AOS was only observed in a limited number of materials systems, all including rare-earth (Gd) transition-metal alloys [2,3,7,8]. Very recently, it was also demonstrated for the synthetic-ferrimagnetic layered structure [9], which allows for easy spintronic integration [10]. The fact that single-pulse AOS is observed in both ferrimagnetic alloys and synthetic-ferrimagnetic multilayers raises the questions to what extent the switching of these materials systems relies on the same physics, and what the specific conditions are for switching these materials systems.

In this work, we show that the conditions for single-pulse AOS in alloys (GdCo) and synthetic ferrimagnets (Co/Gd bilayers) are strikingly different. We experimentally demonstrate that single-pulse AOS in synthetic-ferrimagnetic Pt/FM/Gd is very robust, and can be achieved for a large range of the ferromagnetic (FM) layer thickness. The experiments indicate that the Pt/FM/Gd stacks can be switched in the absence of a compensation temperature. In contrast, for alloys it is believed that it is crucial to have a compensation temperature near ambient temperature, such that the magnetization of the sublattices is compensated significantly [7,11].

We performed simulations in order to understand this contrasting behavior and to identify the underlying mechanisms. The general theoretical framework for AOS describes the dynamics of multiple magnetic sublattices which are coupled antiferromagnetically. The intersublattice exchange coupling plays a crucial role, transferring angular momentum between the sublattices [12]. Different approaches have been made to describe the spin dynamics of the magnetic sublattices, e.g., the atomistic Landau-Lifshitz-Gilbert equation [13–17] and the microscopic three-temperature model (M3TM) [18,19]. Here, we use the latter microscopic description, in which it is assumed that angular momentum transfer between the sublattices is mediated by exchange scattering [19]. We derive an analytical expression for the magnetization dynamics resulting from the exchange scattering between (i) the sublattices in a GdCo alloy and (ii) the atomic monolayers in a Co/Gd bilayer. The model reproduces the distinct role of the compensation temperature. Moreover, it shows that the robustness of AOS in the Co/Gd bilayers can be explained by the nonlocal character of the switching mechanism, which we identify as a front of reversed Co magnetization that propagates away from the interface.

This work starts with a brief description of the experimental methods and results. After that, the theoretical framework will be introduced. For the sake of direct comparison, we focus our theoretical discussion on the magnetization dynamics in GdCo alloys and Co/Gd bilayers. We present phase diagrams that show qualitatively the switching conditions and point out the differences for both materials systems. Finally, the typical switching mechanism of the bilayers is explained explicitly.

The experiments are performed using Si:B(substrate)/Ta(4)/Pt(4)/FM/Gd(3)/Pt(2) stacks (thickness in nanometers), which are deposited at room temperature using dc

*Corresponding author: m.beens@tue.nl

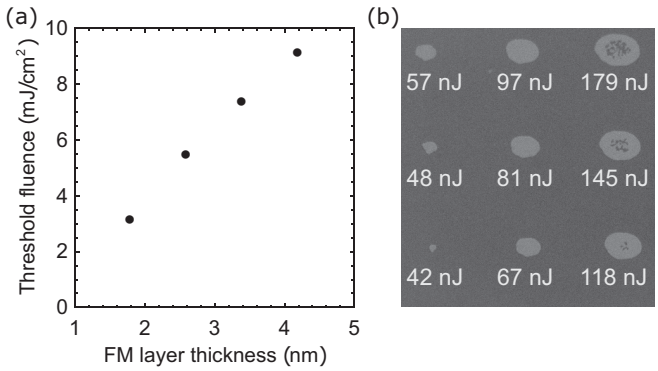

FIG. 1. (a) Threshold fluence as a function of the FM layer thickness in a Pt/FM/Gd stack. The black dots are measured using a FM layer composed of $Co(0.2)/[Ni(0.6)/Co(0.2)]_N$ multilayers for $N = 2, 3, 4, 5$. The error margins are small compared to the scale of the figure. (b) A Kerr microscope image of the (initially saturated) Co/Ni sample with $N = 3$ after excitation with single linearly polarized laser pulses with different pulse energies.

magnetron sputtering at 10^{-8} mbar base pressure. In this work, $Co(0.2)/[Ni(0.6)/Co(0.2)]_N$ multilayers are used for the FM layer, with N repeats ranging from $N = 2$ to 5. Using polar magneto-optical Kerr effect measurements, a square hysteresis loop with 100% remanence was obtained for all samples, confirming the presence of a well-defined perpendicular magnetic anisotropy in the samples.

The response of the magnetization in the Pt/FM/Gd stacks to laser-pulse excitation was investigated using linearly polarized laser pulses with a central wavelength of 700 nm and a pulse duration of ≈100 fs. The measurements are performed at room temperature, and start by saturating the magnetization using an externally applied field. Then, the external field is turned off, and the sample is exposed to single laser pulses with varying pulse energies. The response of the magnetization to the laser-pulse excitation is measured in the steady state (i.e., long after the excitation) using a magneto-optical Kerr microscope.

A typical result of the AOS measurement for the sample with $N = 3$ is presented in Fig. 1(b). The figure displays the Kerr image of the (initially saturated, dark) sample after excitation with single linearly polarized laser pulses with different pulse energies. The figure shows clear homogeneous domains with an opposite magnetization direction (light) being written by the laser pulses. Moreover, the domain size increases for increasing pulse energy, as is expected when using a Gaussian pulse shape. For the highest pulse energies a multidomain state is formed in the center region of the domain, where the lattice is heated above the Curie temperature [20].

The AOS-written domain size as a function of the pulse energy can be used to determine the threshold fluence [9,21]. Figure 1(a) displays the threshold fluence as a function of the (total) thickness of the $Co(0.2)/[Ni(0.6)/Co(0.2)]_N$ multilayer. The results show that decreasing the thickness of the FM layer leads to a lower threshold fluence. This behavior is reproduced in the model calculations that are presented later. It can be partially explained by a decrease in the Curie temperature with film thickness in the thin-film limit, but it will be shown that also other processes are involved.

Remarkably, single-pulse AOS is seen for up to five repeats, corresponding to a FM layer thickness of 4.2 nm. For these relatively thick FM layers, the total magnetic moment of the FM layer is much larger than the induced magnetic moment in the Gd layer corresponding to approximately 1–2 atomic monolayers of fully saturated Gd [9], i.e., the system is far from compensated. Hence, the experiment indicates that the switching mechanism in the bilayers is independent of a possible compensation temperature. To understand the underlying mechanism, we developed a simplified model.

Analogous to Schellekens and Koopmans [19], we assume that separate spin subsystems are coupled to a single electron and phonon subsystem. Like in the basic M3TM [18], the electrons are treated as a spinless free electron gas and the phonons are described within the Debye model. It is assumed that both subsystems are internally thermalized, and that the electron temperature T_e and phonon temperature T_p are homogeneous. The spin specific heat is neglected. Femtosecond laser heating is modeled by adding an energy source to the electron subsystem. Heat diffusion to the substrate is added to the phonon subsystem as an energy dissipation term with timescale τ_D. The spin subsystems, labeled with index i, are treated within a Weiss mean-field approach. At each lattice site $D_{s,i} = \mu_{at,i}/2S_i$ spins are present, where $\mu_{at,i}$ is the atomic magnetic moment (in units of the Bohr magneton μ_B) and S_i is the spin quantum number.

For the $Gd_{1-x}Co_x$ alloys, we define a normalized magnetization m_i for each of the two sublattices. As depicted in the inset of Fig. 2(a), the exchange field experienced by each atom depends on the type of atom and the composition of its nearest neighbors. Hence, the exchange splitting is given by

$$\Delta_{Co} = x\gamma_{Co\text{-}Co}m_{Co} + (1-x)\gamma_{Co\text{-}Gd}m_{Gd}, \quad (1)$$

$$\Delta_{Gd} = x\gamma_{Gd\text{-}Co}m_{Co} + (1-x)\gamma_{Gd\text{-}Gd}m_{Gd}, \quad (2)$$

where we defined $\gamma_{ij} = j_{ij}zD_{s,j}S_j$ ($i, j \in \{Co,Gd\}$) in terms of the (intra- or intersublattice) exchange coupling constant j_{ij} and the number of nearest neighbors z. Note that $j_{Co\text{-}Gd}$ is negative and quantifies the strength of the antiferromagnetic coupling between the Co and Gd sublattices.

For the Co/Gd bilayers we introduce a normalized magnetization m_i for each atomic monolayer i separately. Each layer only interacts with its adjacent layers. For simplicity, we assume that the separate layers lie in the (111) plane of an fcc lattice. This means that each atom has six nearest neighbors in the same layer and three nearest neighbors in each adjacent layer. Thus, the exchange splitting of layer i is

$$\Delta_i = \frac{\gamma_{i,i-1}}{4}m_{i-1} + \frac{\gamma_{i,i}}{2}m_i + \frac{\gamma_{i,i+1}}{4}m_{i+1}. \quad (3)$$

Note that the antiferromagnetic coupling, proportional to $j_{Co\text{-}Gd}$, is only experienced by the layers adjacent to the interface [see inset in Fig. 2(b)].

We include two channels for angular momentum transfer. Elliott-Yafet spin-flip scattering mediates the transfer of angular momentum between the spin subsystems and the lattice [22]. An extension of the M3TM, which accounts for spin systems with arbitrary spin S, is derived to describe the resulting

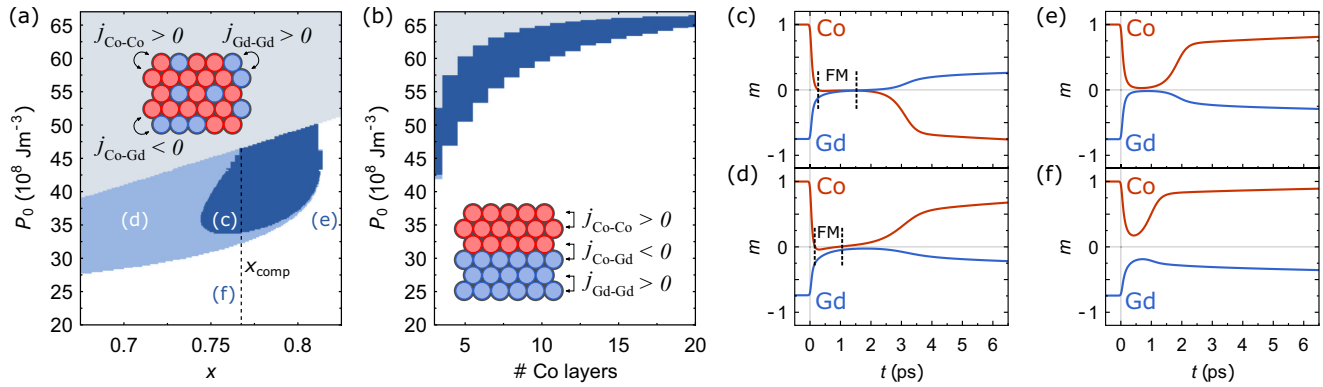

FIG. 2. Phase diagram for AOS as a function of the laser pulse energy P_0 and (a) Co concentration x for a $Gd_{1-x}Co_x$ alloy, and (b) the number of Co monolayers in a Co/Gd bilayer. The dark-blue regions indicate a switch in the final state (c) and the white regions indicate no switch (e),(f). Light blue indicates a transient ferromagnetic state, but no switch (d). The gray regions indicate that the phonon temperature T_p exceeds the Curie temperature T_C. The dashed line in (a) indicates the Co concentration x_{comp} for which the compensation temperature is equal to room temperature. The insets in (a) and (b) schematically show the modeled system, including the exchange parameters. (c)–(f) display the element-specific magnetization dynamics in $Gd_{1-x}Co_x$ for different values for x and P_0, corresponding to the various regions in (a).

magnetization dynamics [18,23,24]. Here, we take $S_{Co} = 1/2$ and $S_{Gd} = 7/2$, for which the Weiss model is well fitted to the experimental data for the magnetization as a function of temperature [25,26]. Angular momentum transfer between the different spin subsystems is mediated by exchange scattering [19]. In this *e-e* scattering process, spins originating from different subsystems are flipped in the opposite direction. We use Fermi's golden rule to find an analytical expression for the magnetization dynamics resulting from the exchange scattering (see Supplemental Material Sec. II) [24]. For $i \neq j$ we have

$$\left.\frac{dm_i}{dt}\right|_{ex} = \frac{2\eta_{ij}C_j}{\mu_{at,i}}T_e^3\left[\sum_{s=-S_i+1}^{S_i}\sum_{s'=-S_j}^{S_j-1} W_{ij;ss'}^{-+}(\Delta_i - \Delta_j)f_{i,s}f_{j,s'} - \sum_{s=-S_i}^{S_i-1}\sum_{s'=-S_j+1}^{S_j} W_{ij;ss'}^{+-}(\Delta_i - \Delta_j)f_{i,s}f_{j,s'}\right]. \quad (4)$$

The indices s and s' correspond to the z component of the spin and label the discrete energy levels. The average occupation of level s in spin subsystem i is given by $f_{i,s}$, and $\Delta_i - \Delta_j$ is the energy difference between the initial and final spin configuration. The dimensionless function $W_{ij;ss'}^{\pm\mp}$ parametrizes the transition rate from level s to $s \pm 1$ in subsystem i and level s' to $s' \mp 1$ in subsystem j. The coordination number C_j counts the relative number of nearest neighbors that are part of spin subsystem j. For alloys C_j is given by $C_{Co} = 12x$ and $C_{Gd} = 12(1-x)$. For bilayers we have $C_j = 3$, the number of nearest neighbors in an adjacent layer. The constant η_{ij} is determined by the matrix element of the exchange scattering Hamiltonian [24], for which we assume that it is proportional to the exchange coupling constant. Hence, we write $\eta_{ij} \propto \lambda_{ij} j_{ij}^2$, where λ_{ij} is a dimensionless parameter. In the following discussions we assume that $\lambda_{ij} = \lambda = 5$, which is chosen in order to retrieve realistic results from the simulations (e.g., for $\lambda = 1$ no switching is found). Results for different choices of λ and S_{Gd} are presented in the Supplemental Material [24].

Note that for the bilayers, Eq. (4) should include terms for the interaction with both adjacent layers, i.e., $j = i + 1$ and $j = i - 1$, and the full expression is given by the sum of these two terms.

The temporal profile of the laser pulse is modeled by a Gaussian function $P(t) = [P_0/(\sigma\sqrt{\pi})]\mathrm{Exp}[-(t-t_0)^2/\sigma^2]$, where P_0 is the absorbed laser pulse energy density and σ is the pulse duration, which is set to 50 fs. We assume that the laser pulse heats up the system homogeneously, which is a valid approximation for the systems we model, e.g., Co/Gd bilayers containing up to 20 Co atomic monolayers. We note that for thicker systems the approximation becomes questionable, and a finite penetration depth should be incorporated into the modeling.

The laser-induced dynamics of $m_i(t)$ is calculated numerically. We assume that the spin subsystems are not necessarily in internal equilibrium, meaning that after excitation the ratio between $f_{i,s}$ and $f_{i,s\pm1}$ is not given by a Boltzmann distribution, and we need to solve a set of $2S_i + 1$ coupled differential equations for each spin subsystem i [24]. The exact values for the material parameters, including the exchange coupling constants j_{ij}, are listed in the Supplemental Material [24].

Two phase diagrams are constructed that display the occurrence of AOS as a function of the laser pulse energy P_0 and (i) the Co concentration x of a $Gd_{1-x}Co_x$ alloy, and (ii) the number of Co monolayers for a Co/Gd bilayer (the Co thickness). We assume that the ambient temperature is equal to room temperature ($T_{amb} = 295$ K). The result is shown in Figs. 2(a) and 2(b). The color scheme indicates whether the magnetization of the Co is reversed after relaxation, which is determined by calculating its sign at $t = 100$ ps. For the bilayers we take the average of the magnetization of the Co monolayers. Figures 2(c)–2(f) are presented to clarify the meaning of the color scheme, and show the corresponding element-specific magnetization dynamics for the alloys. In the phase diagrams, the dark-blue regions indicate that the Co magnetization is reversed, meaning that AOS has occurred [Fig. 2(c)]. The light-blue regions indicate that there

is a transient ferromagnetic state created, but after relaxation the magnetization is switched back to its initial direction [Fig. 2(d)]. The white regions indicate that the magnetization relaxes to its initial direction, without a transient ferromagnetic state [Figs. 2(e) and 2(f)]. The gray regions indicate that the maximum of the phonon temperature T_p exceeds the Curie temperature. In the experiments, this would likely result in the creation of a multidomain state [20].

The vertical dashed line in Fig. 2(a) indicates the compensation point $x_{\mathrm{comp}} \sim 0.77$, the Co concentration for which the total magnetic moment of the alloy is zero at room temperature. The dark-blue region shows that the alloys can only be switched in a limited range of the Co concentration, sufficiently close to the compensation point. Furthermore, the minimum threshold fluence is found to be close to the compensation point. These findings are in agreement with the experiments [11]. From the phase diagram we can conclude that in order to switch the alloy, a significant magnetization compensation is necessary. Hence, the model yields that the magnetization compensation temperature plays a crucial role in switching the alloys.

A clear difference is found when we compare this to the situation for bilayers, Fig. 2(b). This phase diagram shows that the bilayers can be switched for a relatively large number of Co monolayers, even though the threshold fluence increases as a function of the number of Co monolayers. More specifically, even bilayers with 20 Co monolayers can be switched. For these bilayers, the ratio of the total Co and Gd magnetic moment is $\mu_{\mathrm{Co}}/\mu_{\mathrm{Gd}} \sim 4$ (at $T_{\mathrm{amb}} = 295$ K), which is significantly far from compensation ($\mu_{\mathrm{Co}}/\mu_{\mathrm{Gd}} = 1$). In contrast, for the alloys switching only occurs in the range $\mu_{\mathrm{Co}}/\mu_{\mathrm{Gd}} \sim 0.9$–$1.3$. Note that for convenience we described the FM layer as pure Co, whereas in the experiments Co/Ni multilayers are used. Including the Co/Ni multilayers will not change the qualitative properties of the switching mechanism. Hence, the model agrees well with our experimental observation that shows single-pulse AOS in Pt/FM/Gd for relatively thick FM layers, and verifies that the magnetization compensation temperature does not play a crucial role in switching the synthetic ferrimagnets.

A more detailed analysis of the typical switching mechanism in the bilayers is presented in Fig. 3, which shows AOS in a system of 5 Co monolayers and 3 Gd monolayers. We plotted the normalized magnetization of the separate layers as a function of time after laser pulse excitation (at $t = 0$). The inset displays the time at which each Co monolayer reverses its magnetization direction, for a system of 14 Co layers and 3 Gd layers. The inset clearly shows that the Co layers are switched consecutively, starting with the Co layers near the Co/Gd interface. Triggered by the laser pulse, the switch is initiated near the interface due to exchange scattering

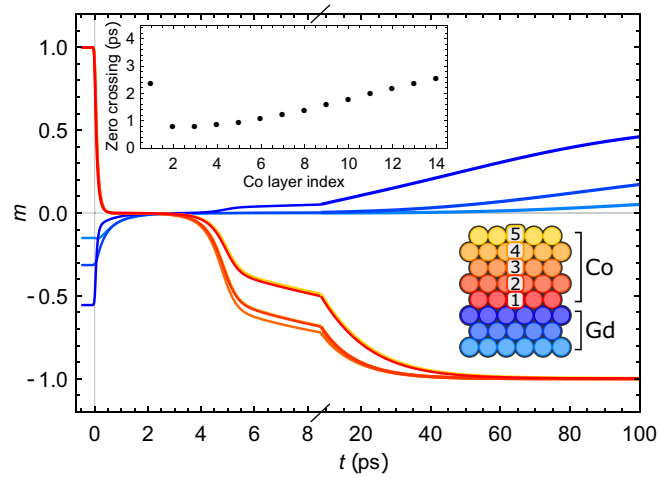

FIG. 3. Laser-induced magnetization dynamics of all atomic monolayers in a Co/Gd bilayer consisting of 5 Co monolayers and 3 Gd monolayers for $P_0 = 55 \times 10^8$ J m^{-3}. The inset shows the time at which the magnetization of each Co monolayer is reversed for a system of 14 Co layers and 3 Gd layers for $P_0 = 65 \times 10^8$ J m^{-3} (index 1 corresponds to the Co layer adjacent to the interface).

between the adjacent Co and Gd monolayers. The dynamics of the first Co monolayer (Index 1 in Fig. 3) is strongly modified by the exchange field from the slowly demagnetizing Gd layer [24]. Hence, the second Co monolayer is switched first. Subsequently, the switch propagates throughout the Co layer driven by exchange scattering between neighboring Co monolayers. This successive switching mechanism, with a front of reversed Co magnetization propagating away from the interface, can succeed independently of the number of Co monolayers and explains why the Co/Gd bilayer can be switched for a relatively large Co thickness.

To conclude, both the experiment and the theoretical model show that single-pulse AOS switching in synthetic-ferrimagnetic bilayers is independent of a possible compensation temperature, whereas in ferrimagnetic alloys the compensation temperature plays a crucial role. We identified the propagation of a switching front as the characteristic mechanism for AOS in the bilayers. These new insights show that single-pulse AOS in synthetic ferrimagnets is more robust than in ferrimagnetic alloys, and emphasize that Pt/FM/Gd synthetic ferrimagnets are a very promising candidate for integration of single-pulse AOS in future data storage devices.

This work is part of the research program of the Foundation for Fundamental Research on Matter (FOM), which is part of the Netherlands Organisation for Scientific Research (NWO).

[1] C. D. Stanciu, F. Hansteen, A. V. Kimel, A. Kirilyuk, A. Tsukamoto, A. Itoh, and Th. Rasing, All-Optical Magnetic Recording with Circularly Polarized Light, Phys. Rev. Lett. **99**, 047601 (2007).

[2] I. Radu, K. Vahaplar, C. Stamm, T. Kachel, N. Pontius, H. A. Dürr, T. A. Ostler, J. Barker, R. F. L. Evans, R. W. Chantrell, A. Tsukamoto, A. Itoh, A. Kirilyuk, Th. Rasing, and A. V. Kimel, Transient ferromagnetic-like state mediating ultrafast reversal of antiferromagnetically coupled spins, Nature (London) **472**, 205 (2011).

[3] T. A. Ostler, J. Barker, R. F. L. Evans, R. W. Chantrell, U. Atxitia, O. Chubykalo-Fesenko, S. El Moussaoui, L. Le

Guyader, E. Mengotti, L. J. Heyderman, F. Nolting, A. Tsukamoto, A. Itoh, D. Afanasiev, B. A. Ivanov, A. M. Kalashnikova, K. Vahaplar, J. Mentink, A. Kirilyuk, Th. Rasing, and A. V. Kimel, Ultrafast heating as a sufficient stimulus for magnetization reversal in a ferrimagnet, Nat. Commun. **3**, 666 (2012).

[4] M. S. El Hadri, P. Pirro, C.-H. Lambert, S. Petit-Watelot, Y. Quessab, M. Hehn, F. Montaigne, G. Malinowski, and S. Mangin, Two types of all-optical magnetization switching mechanisms using femtosecond laser pulses, Phys. Rev. B **94**, 064412 (2016).

[5] S. Mangin, M. Gottwald, C.-H. Lambert, D. Steil, V. Uhlíř, L. Pang, M. Hehn, S. Alebrand, M. Cinchetti, G. Malinowski, Y. Fainman, M. Aeschlimann, and E. E. Fullerton, Engineered materials for all-optical helicity-dependent magnetic switching, Nat. Mater. **13**, 286 (2014).

[6] R. Medapalli, D. Afanasiev, D. K. Kim, Y. Quessab, S. Manna, S. A. Montoya, A. Kirilyuk, Th. Rasing, A. V. Kimel, and E. E. Fullerton, Multiscale dynamics of helicity-dependent all-optical magnetization reversal in ferromagnetic Co/Pt multilayers, Phys. Rev. B **96**, 224421 (2017).

[7] L. Le Guyader, S. El Moussaoui, M. Buzzi, M. Savoini, A. Tsukamoto, A. Itoh, A. Kirilyuk, Th. Rasing, F. Nolting, and A. V. Kimel, Deterministic character of all-optical magnetization switching in GdFe-based ferrimagnetic alloys, Phys. Rev. B **93**, 134402 (2016).

[8] J. Gorchon, C.-H. Lambert, Y. Yang, A. Pattabi, R. B. Wilson, S. Salahuddin, and J. Bokor, Single shot ultrafast all optical magnetization switching of ferromagnetic Co/Pt multilayers, Appl. Phys. Lett. **111**, 042401 (2017).

[9] M. L. M. Lalieu, M. J. G. Peeters, S. R. R. Haenen, R. Lavrijsen, and B. Koopmans, Deterministic all-optical switching of synthetic ferrimagnets using single femtosecond laser pulses, Phys. Rev. B **96**, 220411(R) (2017).

[10] M. L. M. Lalieu, R. Lavrijsen, and B. Koopmans, Integrating all-optical switching with spintronics, Nat. Commun. **10**, 110 (2019).

[11] Y. Xu, M. Deb, G. Malinowski, M. Hehn, W. Zhao, and S. Mangin, Ultrafast magnetization manipulation using single femtosecond light and hot-electron pulses, Adv. Mater. **29**, 1703474 (2017).

[12] J. H. Mentink, J. Hellsvik, D. V. Afanasiev, B. A. Ivanov, A. Kirilyuk, A. V. Kimel, O. Eriksson, M. I. Katsnelson, and Th. Rasing, Ultrafast Spin Dynamics in Multisublattice Magnets, Phys. Rev. Lett. **108**, 057202 (2012).

[13] T. A. Ostler, R. F. L. Evans, R. W. Chantrell, U. Atxitia, O. Chubykalo-Fesenko, I. Radu, R. Abrudan, F. Radu, A. Tsukamoto, A. Itoh, A. Kirilyuk, Th. Rasing, and A. V. Kimel, Crystallographically amorphous ferrimagnetic alloys: Comparing a localized atomistic spin model with experiments, Phys. Rev. B **84**, 024407 (2011).

[14] U. Atxitia, P. Nieves, and O. Chubykalo-Fesenko, Landau-Lifshitz-Bloch equation for ferrimagnetic materials, Phys. Rev. B **86**, 104414 (2012).

[15] J. Barker, U. Atxitia, T. A. Ostler, O. Hovorka, O. Chubykalo-Fesenko, and R. W. Chantrell, Two-magnon bound state causes ultrafast thermally induced magnetization switching, Sci. Rep. **3**, 3262 (2013).

[16] S. Gerlach, L. Oroszlany, D. Hinzke, S. Sievering, S. Wienholdt, L. Szunyogh, and U. Nowak, Modeling ultrafast all-optical switching in synthetic ferrimagnets, Phys. Rev. B **95**, 224435 (2017).

[17] U. Atxitia and T. A. Ostler, Ultrafast double magnetization switching in GdFeCo with two picosecond-delayed femtosecond pump pulses, Appl. Phys. Lett. **113**, 062402 (2018).

[18] B. Koopmans, G. Malinowski, F. Dalla Longa, D. Steiauf, M. Fähnle, T. Roth, M. Cinchetti, and M. Aeschlimann, Explaining the paradoxical diversity of ultrafast laser-induced demagnetization, Nat. Mater. **9**, 259 (2010).

[19] A. J. Schellekens and B. Koopmans, Microscopic model for ultrafast magnetization dynamics of multisublattice magnets, Phys. Rev. B **87**, 020407(R) (2013).

[20] J. Gorchon, R. B. Wilson, Y. Yang, A. Pattabi, J. Y. Chen, L. He, J. P. Wang, M. Li, and J. Bokor, Role of electron and phonon temperatures in the helicity-independent all-optical switching of GdFeCo, Phys. Rev. B **94**, 184406 (2016).

[21] J. M. Liu, Simple technique for measurements of pulsed Gaussian-beam spot sizes, Opt. Lett. **7**, 196 (1982).

[22] B. Koopmans, J. J. M. Ruigrok, F. Dalla Longa, and W. J. M. de Jonge, Unifying Ultrafast Magnetization Dynamics, Phys. Rev. Lett. **95**, 267207 (2005).

[23] Ł. Cywiński and L. J. Sham, Ultrafast demagnetization in the *sp-d* model: A theoretical study, Phys. Rev. B **76**, 045205 (2007).

[24] See Supplemental Material at http://link.aps.org/supplemental/10.1103/PhysRevB.100.220409 for (i) M3TM for systems with an arbitrary spin, (ii) details about exchange scattering, (iii) the exchange scattering rate constant, (iv) used system parameters, (v) notes on the inset of Fig. 3, (vi) phase diagrams for different exchange scattering rates, and (vii) experimental domain size as a function of pulse energy.

[25] B. D. Cullity and C. D. Graham, *Introduction to Magnetic Materials* (Wiley, New York, 1972).

[26] J. M. D. Coey, *Magnetism and Magnetic Materials* (Cambridge University Press, Cambridge, UK, 2009).